Supplementary material for the article "Cross section measurements of ^{155,157}Gd(n,γ) induced by thermal and epithermal neutrons"

In order not to inflate Sec. IV C of the article "Cross section measurements of ^{155,157}Gd(n,γ) induced by thermal and epithermal neutrons", we shortened the text as much as possible and included only the crucial Figures in the article. In this supplementary material we will touch the analysis of statistical properties of neutron resonances in more details. This material is not supposed to be taken as a stand-alone text. Some Figures from the article are repeated for clarity, the references to the Tables and Figures of the article are in bold in present text, while the references to the Tables and Figures of this material are in normal font (and hyperref in pdf).

I. STATISTICAL PROPERTIES OF NEUTRON RESONANCES

A. General remarks related to data processing

As pointed out in the article, the total width of resonances, $\Gamma = \Gamma_n + \Gamma_\gamma$, is strongly dominated by the Doppler broadening at higher neutron energies. The lower limit of Γ is given by the Γ_γ with average value of about 100 meV in both studied nuclei, while the actual values of Γ_γ among different resonances are expected to undergo fluctuations only of a few meV from statistical model calculations. As the neutron width Γ_n is in most cases smaller than Γ_γ, typically by one or two orders of magnitude in the resolved resonance regions (RRR), the FWHM from the Doppler broadening becomes comparable to Γ already at $E_n \approx 10$ eV; for $E_n = 50$ eV it is about $2-3\times$ higher and for $E_n = 200$ eV about $4-6\times$ higher than Γ. The actual energy resolution of n_TOF spectrometer is in the order of tens meV at these energies.

The radiative width Γ_γ was fixed to the average radiative width $\overline{\Gamma}_\gamma$ from our analysis during the SAMMY fitting for all resonances above the RRR, i.e. above 181 and 307 eV in ^{155}Gd and ^{157}Gd, respectively. On the other hand, the Γ_γ was fitted for all resonances below these energies. To estimate the average radiative width listed in the article, we included the resonances only up to 50 eV, that is 28 and 11 resonances in ^{155}Gd and ^{157}Gd, respectively, to avoid the above-mentioned increasing influence of the Doppler broadening and possible bias introduced by chosen model of this effect. More remarks about $\overline{\Gamma}_\gamma$ can be found in Sec. I B 2.

B. Statistical quantities

Resolved resonance parameters from our analysis are listed in **Tables. IV - VII** of the article. For each quantity determined from these parameters – S_0, $\overline{\Gamma}_\gamma$, and D_0 – we will separately specify what ranges of neutron energies were used for obtaining their values and the reasoning behind these different ranges.

1. Neutron strength function

An estimate of the s-wave neutron strength function S_0 was made from reduced neutron widths as

$$S_0 = \frac{1}{\Delta E} \sum_{\Delta E} g_J \Gamma_n^0 \tag{1}$$

where ΔE is the interval of neutron energies which the reduced neutron widths are summed over. The sum goes over resonances of both spins. All resonances in the RRRs, that means up to 181 eV and 307 eV in ^{155,157}Gd, respectively, were taken into account.

Assuming the neutron strength function for p-wave resonances, S_1, is about $1-2\times 10^{-4}$ in Gd nuclei, see e.g. predictions of the optical model in Fig. 2.2 of the Mughabghab Atlas of neutron resonances [1], no p-wave resonance should be observable in our data as these resonances are too weak. This is discussed and to some extent experimentally confirmed in multiplicity sensitive time-of-flight measurement by Baramsai and collaborators [2].

The fact that we do not observe any p-wave resonances is illustrated in Fig. 1, where experimental data for the capture kernel (black squares) are shown together with results from a randomly generated sequence of resonances – resonances corresponding to different neutron orbital momentum are distinguished, s-waves (red full circles), p-waves (blue empty circles). The $S_1 = 1.5\times 10^{-4}$ was assumed in both these figures; the value of S_0 corresponded to the values derived in this work. The Equal prob (dark green line) shows values of kernel for which the probability of the resonance to be s-wave or p-wave is equal. Note that this does not mean that the number of s-waves below the line should be equal to the number of p-waves above the line. The experimental threshold for the observation of a single, well-isolated resonance is surely higher than this Equal prob line. A reasonable estimate of lower limit of experimental threshold is $\approx 3\times$ the Equal prob line. As a result, there is practically zero probability to observe p-wave resonance in the present experiment.

On the other hand, as evident from Fig. 1 and pointed out in Ref. [2], the Porter-Thomas (PT) fluctuations of individual neutron widths almost surely prevent observation of all s-wave resonances, see the red full circles with very low values in the figure. Nevertheless, the contribution of these missing resonances to the sum in Eq. (1)
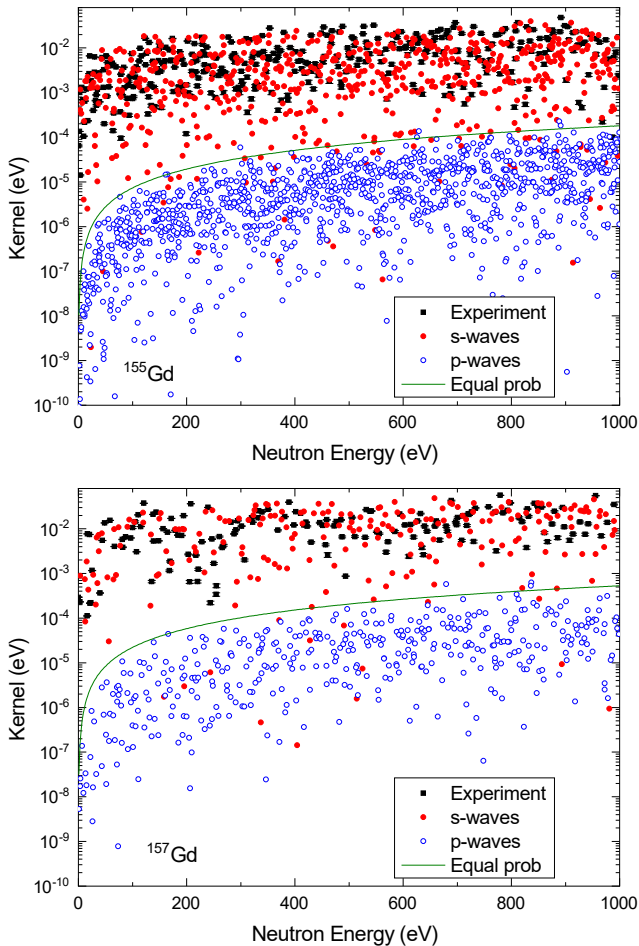
FIG. 1: Resonance kernels for ^{155}Gd (top) and ^{157}Gd (bottom). The experimental data are shown (black squares). There are two randomly generated sequences of resonances - s-waves (red full circles) and p-waves (blue empty circles). The Equal prob (dark green line) shows values of kernel for which the probability of the resonance to be s-wave or p-wave is equal. Note that this does not mean that the number of s-waves below the line should be equal to the number of p-waves above the line. For the explanation of the experimental threshold see Sec. I B 1.

is very small, we expect to miss about 1% of the total strength in the RRR region. The correction for this expected missing strength was applied to get the final values of S_0.

The uncertainty in determination of S_0 is given by the uncertainty in individual Γ_n^0 values from SAMMY fitting and by the PT fluctuations which the Γ_n^0 values are expected to follow. The PT fluctuation adds a relative uncertainty $\sqrt{2/N}$, where $N = \Delta E/D_0$ is the number of all s-wave resonances, D_0 was taken from our analysis, see Sec. I B 3. In the article the corridor in **Fig. 14** is simply given by $S_0 \pm \sigma_{S_0}$, that is fixing ΔE to 181 eV and 307 eV for ^{155,157}Gd, respectively. In Fig. 2 the filled areas are constructed using $N = \Delta E/D_0 = E_n/D_0$ to show what would the uncertainty of S_0 be if we used narrower or
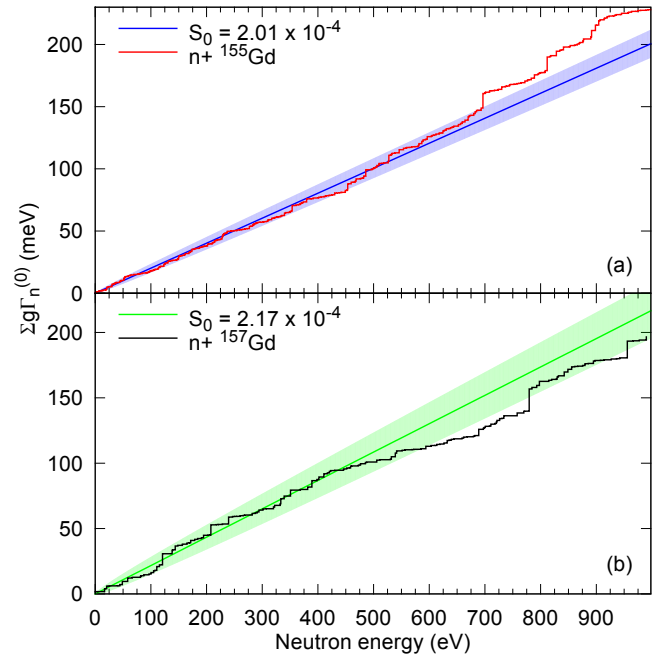
FIG. 2: Cumulative distribution of reduced neutron widths for (a) ^{155}Gd and (b) ^{157}Gd. Solid lines corresponds to deduced S_0 values. The filled areas indicate the 1σ uncertainties (mainly due to Porter-Thomas fluctuations) as described in Sec. I B 1.

wider energy interval ΔE. The dominant contribution to the uncertainty of S_0 comes from the PT fluctuations, experimental uncertainty is negligible. Even if we took region up to 1 keV, the uncertainty from the PT fluctuation is still about 6% and 9.8% in ^{155,157}Gd, respectively, as shown in Fig. 2.

It is worth pointing out that: (a) the experimental data are 3σ compatible within the entire 1 keV range and (b) some of the big steps in the experimental cumulative sequence above RRR might be either due to unresolved doublets (or even more complicated multiplets) or are in reality smaller (thanks to different value of the spin factor g) if the complementary spin was assigned. We remind here that the spins above RRR were assigned randomly only respecting the 3/5 ratio for resonances with $J = 1$ and 2 from the standard spin dependence of the level density.

The experimental data for both nuclei are nicely compatible with either derived S_0. This is illustrated in Fig. 3. The dashed lines in this figure are constructed in the same way as the filled areas in Fig. 2.

2. Average radiative width

The experimental data $\Gamma_{\gamma\lambda}$ for $\lambda = 1, ..., N_{\exp}$ resonances in RRR are shown in Fig. 4 together with the results of the maximum likelihood fit. We stress here that the index λ for labelling individual resonances was
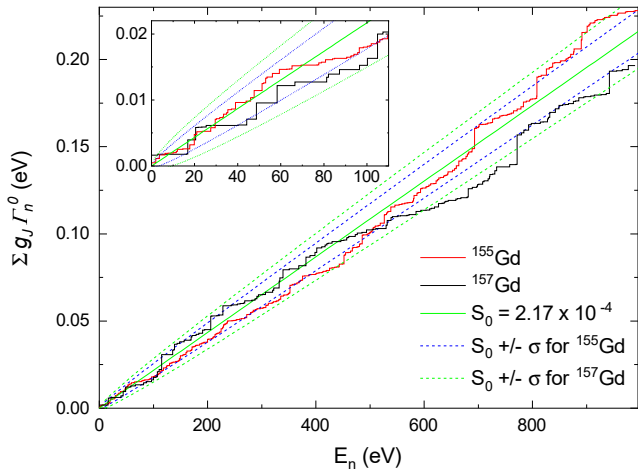
FIG. 3: Cumulative distribution of reduced neutron widths for both Gd nuclei. Solid green line corresponds to $S_0 = 2.17 \times 10^{-4}$ coming from ^{157}Gd data for $E_n < 307$ eV. The dashed lines are constructed in the same way as the filled areas in Fig. 2, see Sec. I B 1 for more details. The red histogram is clearly compatible with blue dashed lines, the black histogram with green dashed lines. Similar figure could be drawn using $S_0 = 2.01 \times 10^{-4}$ coming from ^{155}Gd data for $E_n < 181$ eV.

omitted in the article for the sake of clarity. We assumed that the $\Gamma_{\gamma\lambda}$ values are distributed normally with mean value $\overline{\Gamma}_\gamma$ and with standard deviation σ, so we defined the likelihood function $\mathcal{L}$ as

$$\mathcal{L} = \prod_{\lambda=1}^{N_{\mathrm{exp}}} \frac{1}{\sqrt{2\pi\left(\Delta_\lambda^2 + \sigma^2\right)}} \exp\left(\frac{-\left(\Gamma_{\gamma\lambda} - \overline{\Gamma}_\gamma\right)^2}{2\left(\Delta_\lambda^2 + \sigma^2\right)}\right) h\left(\Delta_\lambda\right), \tag{2}$$

where Δ_λ are uncertainties of individual values $\Gamma_{\gamma\lambda}$ from SAMMY fit and $h\left(\Delta_\lambda\right)$ is the error distribution. We assumed that the error distribution is independent of any other quantity in Eq. (2). This assumption allows us to obtaining results from the likelihood fit without detailed knowledge of this distribution. The experimental error distributions were checked and do not hint any significant dependence.

Using resonances below 50 eV to avoid above-mentioned possible bias due to the Doppler broadening model we obtained $\overline{\Gamma}_\gamma = 106.8(14)$ and $101.1(20)$ meV and $\sigma = 5.9(13)$ and $5.8(18)$ meV for ^{155,157}Gd, respectively. These results are shown as $\overline{\Gamma}_\gamma$ – solid lines and $\overline{\Gamma}_\gamma \pm 3\sigma$ – colored filled area in Fig. 4. Let us repeat the fact that only 30 and 11 resonances were used for the maximum likelihood fit for ^{155}Gd and ^{157}Gd, respectively. The width of the distribution σ is within uncertainty consistent with the value expected from the statistical model for both isotopes.

For comparison with adopted values we give also the results obtained when using all resonances in the RRR: $\overline{\Gamma}_\gamma = 108(2)$ and $105(3)$ meV and $\sigma = 14(2)$ and $19(3)$ meV for ^{155,157}Gd, respectively. The results are shown as shaded filled areas in Fig. 4 covering the re-

gion of $\overline{\Gamma}_\gamma \pm 3\sigma$. The results on $\overline{\Gamma}_\gamma$ are compatible with those obtained with maximum neutron energy of 50 eV for both isotopes while σ is significantly higher. High $\Gamma_{\gamma\lambda}$ values, especially the outliers in ^{157}Gd at resonance energies 104.9 and 171.4 eV, might come from close doublets similar to the one proposed around 37 eV in ^{155}Gd, which are very difficult to resolve. We might also speculate about the influence of the Doppler broadening model as we used resonances from region where the observed width is really dominated by this broadening, see Fig. 9 of the paper. The results from the whole RRR's thus indicate that determination of some radiative widths might not be perfect. However, our main quantity of interest – the resonance kernel – should be determined well even at energies above 50 eV.
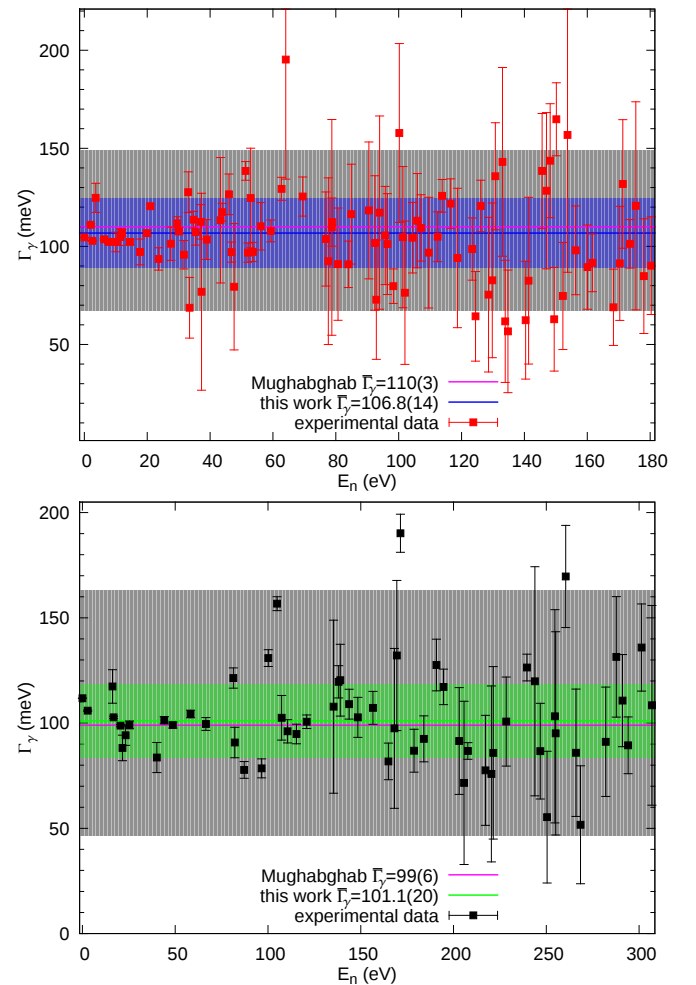

FIG. 4: The radiative width as a function of neutron energy; the upper and lower figures correspond to ^{155}Gd and ^{157}Gd, respectively. The experimental data (points) are plotted with their uncertainties from SAMMY fit. The filled areas correspond to $\overline{\Gamma}_\gamma \pm 3\sigma$, see Sec. I B 2 for explanation.

3. Resonance spacing

The cumulative plot of the number of resonances as a function of neutron energy is shown in Fig. 5. As mentioned above and shown in Fig. 1 the PT fluctuations of individual neutron widths almost surely prevent observation of all s-wave resonances in Gd isotopes from rather low neutron energies, maybe even below 50 eV. Higher number of missing resonance is naturally expected in ^{155}Gd due to lower D_0.
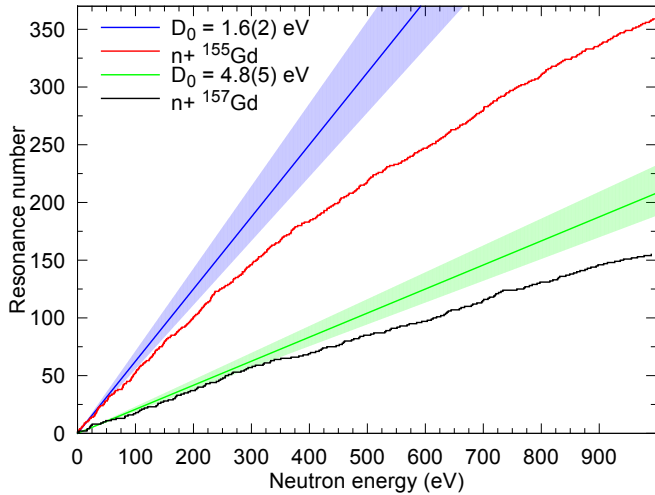

FIG. 5: Cumulative distribution of number of resonances for both Gd isotopes. For the explanation of this plot see Sec. I B 3.

This fact manifests as the global deviation of the number of experimentally observed resonance from the straight line as seen in Fig. 5. The resonance spacing thus can not be calculated as a simple ratio $\Delta E / N_{obs}$, where N_{obs} is the number of observed resonances, but must be corrected for missing resonances. To do that several thousands of artificial resonance sequences were generated using the above-given values of S_0 and $\overline{\Gamma}_\gamma$. Capture kernels of individual resonances were calculated employing the PT fluctuations of generated neutron widths. The number of resonances above a chosen threshold was then compared to experimental value.

Number of observed resonances is for several different artificial thresholds, all of them higher than the estimate of the lower limit of the experimental threshold mentioned in Sec. I B 1, and maximum neutron energies (below 400 eV) nicely consistent (within one sigma corridor) with D_0 in the range about $1.4 - 1.8$ eV and about $4.3 - 5.3$ eV in ^{155}Gd and ^{157}Gd, respectively. These ranges should be close to our estimate of the mean $\pm$ one standard deviation. $D_0 = 1.6(2)$ and $4.8(5)$ eV for ^{155,7}Gd, respectively, are shown as filled areas in Fig. 5. These values are fully consistent with values available in the literature, in particular 1.8(2) eV and 4.47(33) eV from Ref. [1].

We would like mention that we did not test the completeness of the observed resonance sequences (of different lengths) using e.g. Δ_3 statistics. Such test would very likely confirm the results on missing resonances presented in Fig. 1 and would confirm the complete set of resonances only for ^{157}Gd at very low energies.

[1] S. F. Mughabghab, *Atlas of Neutron Resonances*, (Elsevier, Amsterdam, 2006).

[2] B. Baramsai *et al.*, Phys. Rev. C **85**, 024622 (2012).